Cellular automaton modeling of semi-solid microstructure formation

*Li Qiang[1,2], Yu Baoyi[1], Zhang Huawen[1], Li Runxia[1], Wang Feng[1], Xie Shuisheng[2], Huang Guojie[2], and Wang Hao[3]

(1. School of Material Science and Engineering, Shenyang University of Technology, Shenyang 110870, China; 2. State Key Laboratory for Fabrication and Processing of Non-ferrous Metals, Beijing General Research Institute for Non-ferrous Metals, Beijing 100088, China; 3. Faculty of Surveying and Engineering, University of Southern Queensland, Queensland, Australia, 4350)

Abstract: Computer modeling of semi-solid structure formation is of significance in both understanding the mechanisms of globular structure formation and determining the effect of solidification conditions on final microstructure. A modified cellular automaton (mCA) model has been developed, which is coupled with macroscopic models for heat transfer calculation and microscopic models for nucleation and grain growth. The mCA model is applied to A356 Al alloy – one of the most widely used semi-solid alloys, to predict grain morphology and grain size during semi-solid solidification, and determines the effects of pouring temperature on the final microstructure. The modeling results show that the lower the initial temperature, the finer grain size will be obtained. In addition, the model can be used to predict the solutal micro-segregation.

Key words: semi-solid metal processing; microstructure modeling; modified cellular automaton; A356 Al alloy
CLC number: TP391.9 Document code: A Article ID: 1672-6421(2010)02-143-06

Microstructure is a key factor in evaluating the final mechanical properties of semi-solid casting plate. Controlling the size of microstructure to obtain a fine grain microstructure is the aim of semi-solid casting. In the past a lot of researchers have used different experimental methods to obtain fine grains, such as fragmentation of large crystals, electromagnetic stirring, and ultrasonic treatment.

Numerical simulation techniques have the advantages of low cost, high efficiency and ease of being repeated. Therefore, numerical simulation techniques have attracted more and more researchers' interest. Numerical simulation techniques are helpful to better understanding the essence of microstructure and solutal micro-segregation formation during semi-solid casting process. In the past, a lot of numerical methods had been developed, such as theoretical analysis method [1-4], Monte Carlo method [5], Cellular Automaton method [6], Phase Field [7], Front-Tracking method [8] and Level-Set method [9].

Compared with other methods, the Cellular Automaton (CA) method has the advantages of having simple rules, a strong physical background, without restriction by meshed size and not needing to track the topology of the solid/liquid interface. In addition, the CA method has been successful in application to practical solidification [11]. The former researchers [6, 10, 11] who used the CA method to simulate microstructure only considered the thermal diffusing without considering the solute diffusing effects. In 1997, Dilthy et al [12] presented a CA model for both thermal and solutal dendrite based on the thermal and solutal diffusing mechanisms. In 1999 Nastac [13] presented a model combining the thermal diffusion and solutal diffusion together, and the model can be used to simulate the columnar-to-equiaxial transition and show the interaction among the growth dendrites. In 2003, Beltran-Sanchez et al [14] modified the calculating method of the solid/liquid interface curvature in a local meaning to replace the method of counting the solid fraction of the nearest neighbour cells adopted by Dilthy et al [10-13]. In order to overcome the weakness of the former curvature calculating method, Jacot and Rappaz combined the Thermal-Calc software with a CA model to calculate the solid fraction in multi-component alloy solidification [15], which they called pseudo-front tracking method that in essence is a CA method, in which the solid fraction of the solid/liquid interface unit is obtained by Thermal-Cal software according to the local solute concentration, temperature and curvature of the mushy zone; and the interface curvature is calculated by a complex algorithm.

Now our research team has adopted a modified CA method to predict the microstructure and solute micro-segregation of

***Li Qiang**

Male, born in 1973, Ph.D, associate professor. He graduated from Shenyang University in 1994, and obtained the master's and doctor's degree from Northeastern University in 2000 and Institute of Metal Research, Chinese Academy of Science in 2004, respectively. His research interest is on numerical simulation of material processing.
E-mail: solidification@163.com
Received: 2009-06-19; Accepted: 2009-10-20

Al-Si binary alloy during a semi-solid process. In this paper, the mechanism of solute diffusing controlled growth will be adopted, and the curvature of the solid/liquid interface will be found according to the curvature definition. In addition, in order to accelerate the calculating efficiency, the solute potential is adopted to calculate the solute diffusion.

1 Mathematical physical model

The model is based on the following assumptions:

(1) The density of the alloy is assumed to be a constant, which is not changed during the solidification process;

(2) There exists a local phase equilibrium state in the solid-liquid mushy zone;

(3) The influences of liquid convection are ignored;

(4) There are only three kinds of phase states, solid, liquid and the solid/liquid interface where the solid fraction ranges from zero to one. While the solid fraction is zero, its phase state is liquid. When the solid fraction is one, its phase state is solid. Between zero and one, its phase state is solid/liquid interface. In addition, the solid/liquid interface must lie between the solid and liquid unit.

1.1 Energy conservation model

Heat diffusion equation:

$$\frac{\partial T}{\partial t}=\nabla\cdot(\alpha\nabla T)+Q \tag{1}$$

Where T is temperature, t is time, α is the thermal diffusion coefficient, $\alpha=\frac{k}{\rho C_p}$, k is the conductivity, ρ is density, C_p is the specific heat, and Q is the latent heat released as the solid/liquid interface advances into the under-cooled liquid.

$$Q=\frac{\partial f_s}{\partial t}\frac{L_h}{C_p} \tag{2}$$

Where f_s is the solid fraction of the solid/liquid interface zone and L_h is the latent heat released per volume.

1.2 Solute conservation model

Solute diffusion governing equation:

$$\frac{\partial C_I}{\partial t}=\nabla\cdot(D_I\nabla C_I) \tag{3}$$

Where I stands for solid or liquid phase, C is the solute concentration, ∇ is divergence in 2-dimension. In order to simplify the solute diffusion governing equation, Eq.(3) is rewritten as follows:

$$\frac{\partial \overline{C}}{\partial t}=\nabla D_E(\nabla P) \tag{4}$$

Where P is the solute potential, $\overline{C}$ is the averaged solute concentration, D_E is equivalent solute diffusion coefficient, which can be expressed as follows:

$$D_E=\frac{(f_s^i D_s+(1-f_s^i)D_l+f_s^{i+1}D_s+(1-f_s^{i+1})D_l)}{2} \tag{5}$$

Where i and i+1 are the two neighbour units; D_s and D_l are solute diffusing coefficient in solid (s) and liquid (l) phases, respectively. The solute potential can be expressed as follows:

$$\begin{cases}P=C_l & f_s=0\\ P=C_s/k_p & f_s=1\\ P=C_l^* & 0<f_s<1\end{cases} \tag{6}$$

The average solute concentration can be described as follows:

$$\overline{C}=f_s\cdot C_s+(1-f_s)\cdot C_l \tag{7}$$

As the solidification continues, the solute will be redistributed ahead of the solid/liquid interface,

$$C_s^*=k_pC_l^* \tag{8}$$

Where * stands for the solid/liquid interface unit and k_p is the solute partition coefficient ahead of the solid/liquid interface.

1.3 Nucleation model

The continuous nucleation model was adopted according to the Gauss distribution, which can be expressed as:

$$n(\Delta T)=\int_0^{\Delta T}\frac{d_n}{d(\Delta T')}d\Delta T' \tag{9}$$

Where

$$d_n=\frac{n_{\max}}{\sqrt{2\pi}\Delta T_\delta}\exp\left[-\frac{1}{2}\left(\frac{\Delta T-\Delta T_{mn}}{\Delta T_\delta}\right)^2\right] \tag{10}$$

Where $n_{\max}$ is the maximum density of nucleation, ΔT_{mn} is the nucleation under-cooling, ΔT_δ is the standard deviation. For each cell it will generate a random number ranging between zero and one, if the random number is less than the nucleation possibility, the liquid cell will turn into an interface cell; otherwise it will preserve its state.

1.4 Growth model

The solute diffusion controlled growth mechanism is adopted, which means that the advancing velocity of the solid/liquid interface can be got from the solute concentration gradient on both sides of the solid/liquid interface. Therefore, the growth rate of the solid/liquid interface can be written as follows:

$$V=[D_s(\frac{\partial C_s}{\partial n})_s-D_l(\frac{\partial C_l}{\partial n})_l]/(C^*(1-k_p)) \tag{11}$$

Eq. (11) can be made discrete as follows:

$$\begin{aligned}V_x^*&=\frac{1}{C_l^*(1-k)}[-D_L\frac{\partial C_L}{\partial x}|_{\text{int erface}}+D_S\frac{\partial C_S}{\partial x}|_{\text{int erface}}]\\ V_y^*&=\frac{1}{C_l^*(1-k)}[-D_L\frac{\partial C_L}{\partial y}|_{\text{int erface}}+D_S\frac{\partial C_S}{\partial y}|_{\text{int erface}}]\end{aligned} \tag{12}$$

Where V_x and V_y are the interface velocity in horizontal and vertical direction. Discreteness is achieved using forward and backward finite differences with respect to the interface cell of second-order accuracy. The solid/liquid interface is treated as a boundary condition. The discreteness of the composition gradient at the interface in the x-direction is given as the following expressions.

$$\frac{\partial C_L^*}{\partial x}|_{\text{int erface}} = -(\frac{-3C_L^*(i,j)+4C_L(i+1,j)-C_L(i+2,j)}{2dx})F(f_L(i+1,j),\ f_L(i+2,j))+$$
$$(\frac{3C_L^*(i,j)-4C_L(i-1,j)+C_L(i-2,j)}{2dx})F(f_L(i-1,j),\ f_L(i-2,j))$$
$$\frac{\partial C_S^*}{\partial x}|_{\text{int erface}} = -(\frac{-3kC_L^*(i,j)+4C_S(i+1,j)-C_S(i+2,j)}{2dx})F(f_S(i+1,j),\ f_S(i+2,j))+ \quad (13)$$
$$(\frac{3kC_L^*(i,j)+4C_S(i-1,j)+C_S(i-2,j)}{2dx})F(f_S(i-1,j),\ f_S(i-2,j))$$

Where $F(f1, f2)$ is a function that equals zero only when $f1$ and $f2$ all equal zero, otherwise, it equals one. f_s and f_l are solid and liquid fraction, respectively. The solid fraction of interface unit can be deduced as follows:

$$\delta f_s = (v_x + v_y - v_x v_y \cdot \frac{dt}{a})\frac{dt}{a} \ ; \ f_s^n = f_s^{n-1} + \delta f_s \quad (14)$$

Where δf_s is the increase of solid fraction in the solid-liquid interface zone, f_s^n is the solid fraction at the nth time step, and f_s^{n-1} is the solid fraction at the (n-1)th time step, and a is the size of the meshed grid.

Ahead of the solid/liquid interface unit, the relationship between temperature, solute concentration and curvature can be expressed as:

$$T^* = T_{eq} + m(C_l^* - C_0) - \Gamma K f(\theta,\phi) \quad (15)$$

Where T_{eq} is the equilibrium temperature, m is the liquid slope, C_0 is the initial solute concentration, Γ is Gibbs-Thomson coefficient, $f(\theta, \phi)$ is anisotropic function of solid/liquid interface, and K is the curvature of the solid/liquid interface, which can be expressed as follows:

$$K = \frac{z''}{(1+z'^2)^{3/2}} \quad (16)$$

Where

$$z' = \frac{dy}{dx} = \frac{df_s/dx}{df_s/dy} = \frac{(f_s)_x}{(f_s)_y} \quad (17)$$

$$z'' = \frac{d(y')}{dx} = \frac{df_s/dx}{df_s/(dy')} = \frac{(f_s)_x^2(f_s)_{yy}+(f_s)_y^2(f_s)_{xx}-2(f_s)_x(f_s)_y(f_s)_{xy}}{(f_s)_y^3} \quad (18)$$

$$K = \frac{z''}{(1+z'^2)^{3/2}} = \frac{2(f_s)_x(f_s)_y(f_s)_{xy}-(f_s)_x^2(f_s)_{yy}-(f_s)_y^2(f_s)_{xx}}{((fs)_x^2+(fs)_y^2)^{3/2}} \quad (19)$$

The $f(\theta, \phi)$ can be expressed as follows:

$$f(\theta,\phi) = 1 + \delta\cos(4(\phi - \theta)) \quad (20)$$

Whereθ is preferential growth direction of Al-Si alloy crystal, and ϕ is the normal growth direction. The normal angle of the interface is given by:

$$\phi = \arctan(\frac{V_y}{V_x}) \quad (21)$$

The preferential growth direction is a random function which has a value between zero and one. V_x and V_y can be got from Eq. (12). At the beginning of solidification, V_x and V_y are equal to zero, at this time it is assumed $\phi = 0$.

The interface solute concentration, which can be deduced from Eq. (15), is

$$C_l^* = C_0 + \frac{(T^* - T_{eq} - \Gamma\overline{K}f(\theta,\phi))}{m} \quad (22)$$

The interface growth process is also the process of solid fraction increasing in each time step. When the interface is completely solidified, it will capture the neighboring liquid cell to become the interface cell and adopt the neighboring cell's phase state number as its phase state number. The capturing rule of CA can be seen in the work of Sanchez and Stefanescu[14].

The time step is an important factor affecting the calculating efficiency, which can be calculated according to the following equation:

$$\delta t \le \frac{1}{5}Min(\frac{a^2}{D_l},\frac{a^2}{D_s},\frac{a^2}{q_l},\frac{a^2}{q_s},\frac{a}{V_{\max}}) \quad (23)$$

Where Min is a function for selecting the minimum value among $\frac{a^2}{D_l}$, $\frac{a^2}{D_s}$, $\frac{a^2}{q_l}$, $\frac{a^2}{q_s}$ and $\frac{a}{V_{\max}}$, δt is time step, V_{max} is the maximum velocity in the all solid/liquid interface unit, 1/5 means that the advancing interface can't move over 1/5 of meshed grid in each time step.

The calculation steps are given as following:

(1) Setting the initial and boundary conditions;

(2) Calculating the time step according to Eq. (23);

(3) Calculating the temperature field according to Eq. (1);

(4) Calculating the interface curvature according to Eq. (19);

(5) Calculating the interface solute concentration according to Eq. (22);

(6) Calculating the advancing velocity according to Eq. (11);

(7) Calculating the solid fraction according to Eq. (14);

(8) Calculating the solute concentration according to Eq. (3);

(9) Re-assigning the variables, such as temperature, solute concentration, curvature and solid fraction;

(10) Repeating the above steps until reaching the appointed calculating number.

In this study Al-7wt.%Si binary alloy was used as the simulated material, and the parameters used are listed in Table 1.

2 Results and discussion

The whole simulated zone is 0.25 mm × 0.25 mm, which is

Table 1: The parameters used in the model [13]

Parameters	Value
Density (kg/m^3)	2550
Heat diffusion coefficient (m^2/s)	6.1e-6
Solute diffusion coefficient in liquid phase (m^2/s)	1e-9
Solute diffusion coefficient in solid phase (m^2/s)	1e-12
Latent heat (kJ/kg)	270
Specific heat (J/kg•K)	800
Liquidus slope in equilibrium condition	-6
Gibbs-Thomson coefficient (m•K)	9e-8
Partition coefficient in equilibrium condition	0.117
Melting temperature (℃)	660
Solidus (℃)	577

divided into 62,500 meshed grids, and the size of each grid is 1 μm × 1 μm (the meshed grid size should be smaller than the radius of the dendritic tip).

Figure 1 shows the Si concentration distribution when the solidification time is 0.55 s where the initial liquid temperature is 640 ℃. From Fig.1(a) it can be seen that at the grain boundary the Si concentration is very high, and Si concentration accumulates at the grain boundary. In addition, the Si concentration can also affect the microstructure morphology. Due to the solute partition coefficient of Si is very small, only 0.117, as the liquid turns into solid, it will reject most of the Si to the surrounding liquid phase. When most of liquid units have solidified, the remnant liquid will contain a much higher Si concentration, as seen in Fig. 1(a), in which the white spot is the Si concentration higher than 11.5 %. Figure 1(b) indicates the Si solute concentration distribution along a random line, which can reflect where the Si-rich zone and the Si-poor zone are. In Fig. 1(b) it can be seen that the maximum Si solute concentration reaches about 47.5%. According to theoretical calculation, the maximum Si concentration can reach C_0/k_p. Therefore, when the remnant liquid solidifies, the Si concentration will rise up to be about 60%. At the beginning of the simulation, the whole simulated zone is liquid phase and its color is black. When the solidification time is 0.55 s, in Fig. 1(c), there are lots of different color zones in the whole simulated zone and the different color zone stands for different grain size. In this model we adopt 50 different colors to reflect different grain size, which is generated randomly when a liquid turns into solid phase. Using this method not only the Si concentration distribution can be predicted during solidification, but also the final grain size of the microstructure can be predicted. Figure 1(d) is the metallographical image of A356 at a pouring

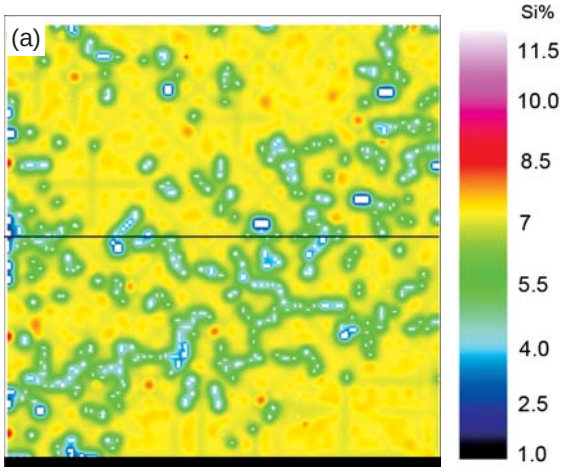

(a) Si concentration distribution at 0.55 s in two dimensions

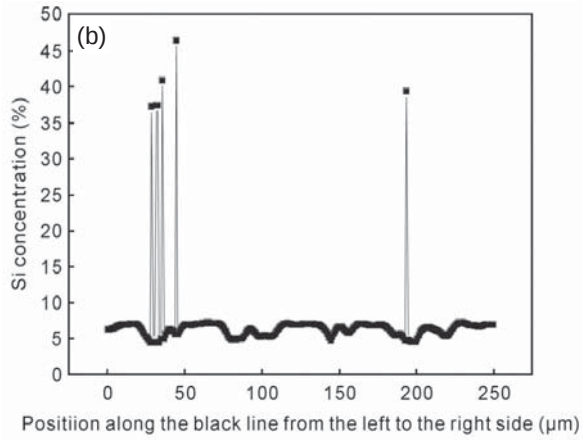

(b) Si concentration distribution along the black line in (a)

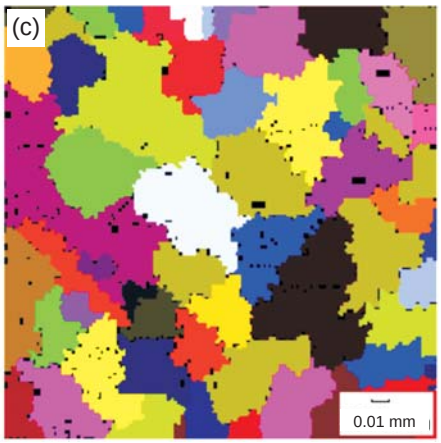

(c) The simulated morphology at 0.55 s

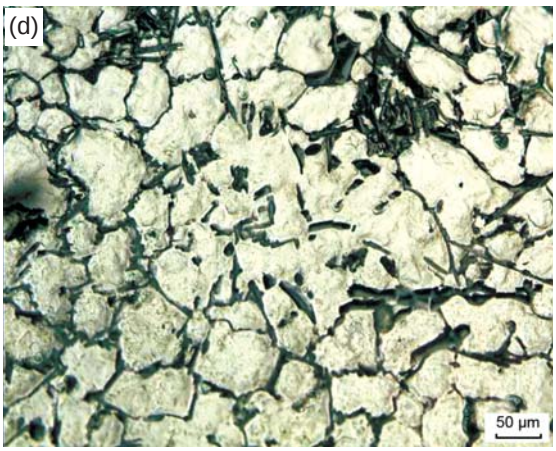

(d) Experimental result

Fig. 1: Si concentration distribution and grain morphology at 0.55 s where the initial liquid temperature is 640 ºC

temperature 640 ℃, which indicates that the morphology and grain size of the simulated results are similar to the experimental results.

Figure 2 shows the Si concentration distribution when the solidification time is 0.012 s where the initial liquid temperature is 620 ℃. Figure 2(a) indicates that at 0.012 s, there are still some zones where the liquid Si concentration is much higher than 11.5 %, which lie at grain boundaries or in the remnant liquid zone. It can be deduced that as the solidification time increases continuously, the difference of Si concentration in the whole zone will decrease. During the solidification process, there is interaction among the grains' growth, which leads to grain growth rate decrease in some directions. Figure 2(b) reflects the Si concentration distribution along the black line in Fig. 2(a), and it can be seen that the maximum Si concentration is about 32.5%, and the lowest Si concentration is about 2.5%. Comparing Fig. 2 with Fig. 1, it can be found that as the solidification time increases the Si concentration in remnant liquid will increase, which decreases the liquidus and therefore the remnant liquid does not easy to solidify.

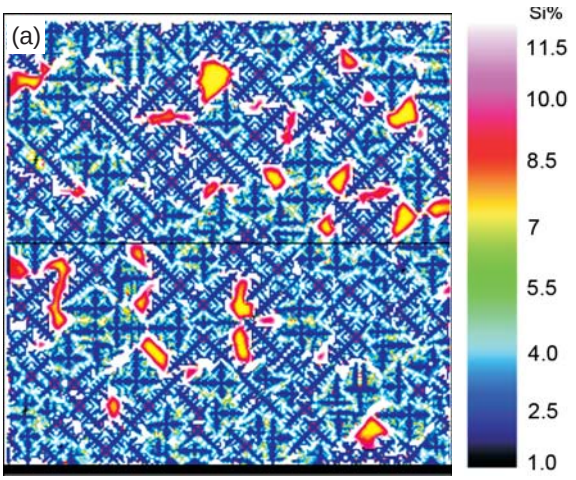

(a) Si concentration distribution at 0.012 s

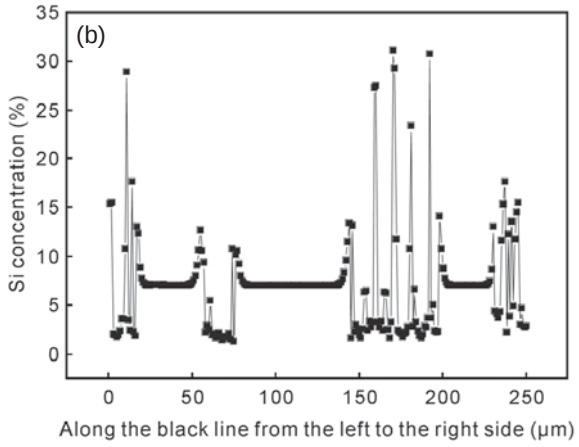

(b) Si concentration distribution along the black line in (a)

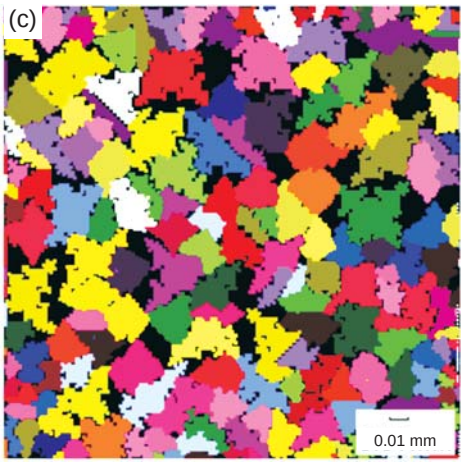

(c) Simulated result

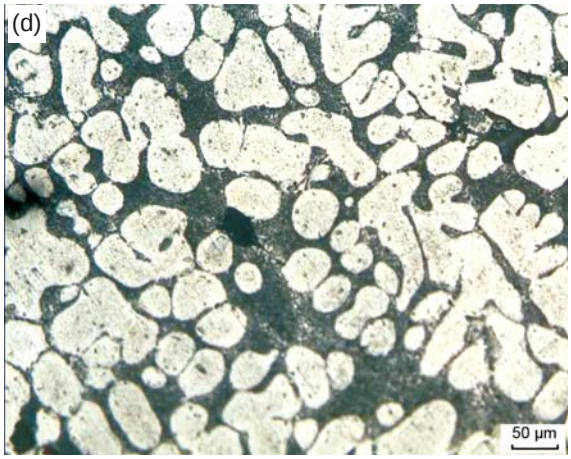

(d) Experimental result

Fig. 2: Si concentration distribution and grain size as solidification time is 0.012 s and initial liquid temperature is 620 ºC.

Figure 2 indicates the grain size at a solidification time 0.012 s, in which the different color stands for the different grain size. Figure 2(c) shows that the grain size is small and averages about 0.03 mm; which is close to the experimental results shown in Fig. 2(d). Comparing Fig. 2 with Fig. 1, it can be found that the grain size in Fig. 2 is much smaller than that in Fig. 1. The reason for this phenomenon is that there are many more nuclei formed in Fig. 2 than in Fig. 1. In addition, it can be seen in Fig. 2 that there are still some black zones, which means that these zones are still in the liquid state.

3 Conclusions

Through simulation, the following conclusions can be drawn:

(1) During the solidification process, Si will be accumulated at the grain boundary, where the maximum Si concentration can reach about 47.5 %, much higher than the initial Si concentration.

(2) The method can be applied to predict the final Si concentration distribution and the final grain size. As the solidification time increases, the Si concentration in the solid phase increases due to back-diffusion.

(3) When the initial temperature is 620 ºC, more nuclei form

than when the initial temperature is 640 ºC, which leads to much smaller grain size.

References

[1] Amar B and Brener E A. Theory of pattern selection in 3-dimension non axisymmetric dendritic growth. Phys. Rev. Lett., 1993, 71: 589–592.

[2] Brener E A. Needle-crystal solution in 3-Dimensional dendritic growth. Phys. Rev. Lett., 1993, 71: 3653–3656.

[3] Brener E A. Three dimensional dendritic growth. J. Cryst. Growth, 1996, 166: 339–346.

[4] McFadden G B, Coriell S R and Sekerka R F. Analytic solution for a non-equilibrium segregation. J. Cryst. Growth, 2000, 208: 726–745.

[5] Spittle J A and Brown S G R. Computer simulation of the effects of alloy variables on the grain structure of casting. Acta Metal., 1989, 37: 1803–1810.

[6] Gandin C A and Rappaz M. Probabilities modeling of microstructure formation in solidification processes. Acta Metal Mater., 1993, 41: 345–360.

[7] Karma A and Rappel W J. Phase field of dendritic side-branching with thermal noise. Phys. Rev. E., 1999, 60: 3614–3625.

[8] Juric D and Tryggvason G. A front tracking method for dendritic solidification. J. Comput. Phys., 1996, 123: 127–148.

[9] Kim Y T, Goldenfeld N, and Dantzig J. Computation of dendritic microstructures using a level set method. Phys. Rev. E., 2000, 62: 2471–2474.

[10] Sasikumar R and Sreenivisan R. Two dimensional simulation for dendritic morphology. Acta Mater., 1994, 42: 2381–2386.

[11] Zhu M F, Kim J M, and Hong C P. Modelling of globular and dendritic structure evolution in solidification of an Al-7mass%Si alloy. ISIJ Inter., 2001, 41: 992–998.

[12] Dilthey U, Pavlik V, and Reichel T. Numerical simulation dendritic solidification with modified cellular automata. In: Proceeding of the Mathematical modelling of welding phenomena conference. Cerjak H and Bhadesia H K D H (Eds.). The Institute of Material, The University of Cambridge, UK. 1997: 85–105.

[13] Nastac L. Numerical modelling of solidification morphologies and segregation patterns in cast dendritic alloys. Acta Mater., 1999, 47: 4253–4262.

[14] Sanchez L B and Stefanescu D M. Growth of solutal dendrites: a cellular automaton model and its quantitative capabilities. Metal Mater. Trans. A, 2003, 34A: 367–382.

[15] Jacot A and Rappaz M. A pseudo-front tracking technique for the modeling of solidification microstructures in multi-component alloys. Acta Mater., 2002, 50: 1909–1926.